



2009 NATIONAL TECHNICAL CONFERENCE & EXHIBITION,  
NEW ORLEANS, LOUISIANA

## AADE 2009-NTCE-12-02: MODELLING THE GELLING PROPERTIES OF WATER-BASED DRILLING FLUIDS

AHMADI TEHRANI, M-I SWACO  
ANDY POPPLESTONE, M-I SWACO

### ABSTRACT

Rheology of drilling fluids affects the frictional pressure drop and the solids carrying capacity of the fluids during the drilling operation. Drilling fluid rheology is commonly controlled by using a variety of clay or polymeric materials, depending on the type of fluid used and the demands of the specific drilling operation. Most drilling fluids possess varying degrees of time- and shear-dependent thixotropic properties. Among them, water-based fluids containing clays, such as bentonite, exhibit a pronounced thixotropic behaviour. This characteristic can have a significant effect on the peaks and troughs of pressure that occur in the wellbore when the drillstring or the tool-string is moved in and out, or when pumping starts after a break in circulation. Major pressure fluctuations can lead to fracturing of the formation, loss of circulation, influx of formation fluids into the wellbore, or collapse of the wellbore. Thus, a practical means of accounting for thixotropy in hydraulics calculations would be of great value for maintaining safety as well as the integrity of the wellbore.

A simple model, based on the concept of a structure parameter, is used to describe drilling fluid thixotropy. Empirical relationships are devised that can predict the time- and shear-dependence of rheological parameters within the range of shear rates encountered inside the drillstring and in the annulus of the wellbore. The model has potential for use in drilling hydraulics calculations.

### Introduction

For drilling fluids to perform satisfactorily, frictional pressure drop and solids-bearing capacity must be maintained at an optimum level throughout the drilling operation. The rheological parameters that control these properties are viscosity and yield stress. Efficient pumping requires a low enough viscosity while adequate yield stress is needed to maintain cuttings in suspension, particularly during circulation breaks.

Drilling fluid rheology is commonly controlled by using a variety of clay or polymeric materials, depending on the type of fluid used and the demands of the specific drilling operation. Of the various types of drilling fluids, water-based muds (WBM) containing clays, such as bentonite or other active particulates such as mixed metal oxides or hydroxides, exhibit a pronounced time and shear dependence. The clay-based fluids are suspensions of bentonite in water to which weight material and other compounds are added to control various drilling fluid properties. The suspended particles are thin, flat platelets that are electrically charged and interact to form a loose “house-of-cards”

structure that is responsible for the gelling characteristics of the fluid when at rest, and its thinning behaviour when sheared.<sup>1</sup> This structure and the resulting bulk rheological properties are time- and shear-history dependent and the fluid is said to possess thixotropic properties.

The rheological properties of the drilling fluid are subject to continuous modification as the fluid circulates around the wellbore. The changes are caused by shearing, temperature, pressure, as well as chemical modification of the fluid as it contacts various formations on its way to the surface.<sup>2</sup>

The shear rates to which the fluid is subjected can range from around  $10^3 \text{ s}^{-1}$  in the drillstring (as the mud travels down the well), to  $\sim 10^5 \text{ s}^{-1}$  in the highly turbulent flow as the fluid issues from the drill bit, to those prevalent in the annulus, *i.e.*  $\sim 10^2 \text{ s}^{-1}$ , as it carries the drill cuttings to the surface.

The combination of temperature, pressure, composition, and time- and shear-history dependence makes a full characterisation of the drilling fluid rheology an extremely complex task. A number of studies have been reported on the temperature, pressure and composition dependence of water-based drilling fluids,<sup>2-5</sup> but only few references exist in the literature on attempts to quantify the thixotropic behaviour of such fluids. Mercer and Weymann<sup>6</sup> investigated the time dependence of viscosity in bentonite-water suspensions and observed that it can be described by a double-exponential function. More recently, Dolz *et al.*<sup>7</sup> investigated the thixotropic behaviour of WBM containing bentonite, at 6-12 wt% concentration, and a polymeric material. They found that the lower concentrations of bentonite produced the greatest thixotropic effect. They obtained an empirical equation that relates shear stress to shear rate, the concentrations of the thickeners and the mixing time.

To improve the quality of downhole predictions requires some form of engineering relationship that can describe the time- and shear-history dependence of rheological properties in drilling fluids. As far as can be determined, the thixotropic characteristics of drilling fluids have not been quantified for engineering applications. Currently, some of the more advanced hydraulics modelling calculations account for this effect by using the so-called “gel” values that are measured by the standard oilfield viscometric method. In this method, the shear stress of the fluid is measured at a low shear rate ( $5.1 \text{ s}^{-1}$ ) after a 10-sec, 10-min, and sometimes 30-min rest period following a short interval of shearing at a high rate. These measurements are used to ensure that the fluids have non-progressive gels, *i.e.* where the longer-term gels are not significantly higher than the 10- or 30-min gel values. This approach has proved to be adequate for most of the applications encountered to date.

However, as drilling scenarios become more complex, a need for a better way of accounting for the thixotropy of drilling fluids will inevitably arise. An example of this is in depleted-zone drilling where the operating window for mud weight (the maximum and minimum mud weights dictated by the pore pressure and fracture gradient considerations) becomes very narrow. In such circumstances, a more detailed knowledge of fluid thixotropy may help to better control drilling hydraulics.

The work reported here uses a simple model based on the concept of a structure parameter to describe drilling fluid thixotropy. Empirical relationships are devised that can predict, with good approximation, the

time- and shear-dependence of rheological parameters within the range of shear rates encountered in the drillstring and the annulus. The model requires further development but shows potential for use in hydraulics calculations.

### Thixotropic Flow Behaviour

Thixotropic materials are fluids containing some form of structure as a result of the formation of flocs or aggregates between suspended particles. In clay suspensions, the formation of structure is promoted by increased encounter between suspended particles, which can result from Brownian motion of the particles or from the velocity gradient when the bulk of the material is sheared. Structure breakdown can be due to collision of particles and flocs, as well as viscous drag exerted by the liquid medium when the material is sheared. On a smaller scale, the Brownian motion of primary particles making up a floc can also cause floc breakup. This means that under certain conditions both Brownian motion and shear can cause structure breakdown. Thixotropic behaviour occurs when the buildup effect of Brownian motion is dominant over the breakdown effect of shear.

When a thixotropic material is sheared, the buildup and breakdown processes compete and a dynamic equilibrium eventually results. Since the rates of buildup and breakdown of structure are finite, if conditions are displaced from equilibrium (e.g. by a change in shear rate), the structure level will take some time to adjust. The change in structure will be detected by a corresponding change in shear stress. This is illustrated in the shear-rate step-change experiments of Fig. 1.

Thixotropic behaviour may also be observed by ramping the shear rate up or down and recording the resulting changes in shear stress (Fig. 2). The breakdown of structure, which occurs as shear rate is increased along the “up” curve, is not fully recovered during the “down” curve and the material completes the cycle with some residual broken structure. The area enclosed between the “up” and “down” curves (the hysteresis loop) is an indication of the extent of thixotropy of the material. If the material is now left to rest, the broken structure will gradually re-form. However, if it is subjected to successive ramping cycles until two consecutive loops superpose, then there is no further drop in the level of structure and the loop is called the equilibrium loop. Another characteristic of such rheograms is the equilibrium flow curve. This is obtained by allowing the material to reach equilibrium structure level at each new shear rate such that the “up” and “down” curves superpose and there is no hysteresis.

The rate and extent of these changes are the parameters that describe thixotropic behaviour and which can be determined by appropriate rheological experiments.

### Structure Theory

In order to obtain a qualitative description of thixotropic behaviour above yield point, a theory involving a single structure parameter  $\lambda$  has been developed which makes use of the concept of some rheological structure at the molecular and particulate level.<sup>8,9</sup> The theory uses two equations to describe single-structure thixotropic behaviour, a rate equation describing structure breakdown and buildup as a function of shear rate and  $\lambda$ :

$$\frac{d\lambda}{dt} = g(\dot{\gamma}, \lambda), \quad (1)$$

and an equation of state relating shear stress to shear rate and structure parameter  $\lambda$ :

$$\tau = \tau(\dot{\gamma}, \lambda) \quad (2)$$

The simplest form of rate equation for structure breakdown and buildup at constant shear rate is given by Moore:<sup>9</sup>

$$\frac{d\lambda(t)}{dt} = \underbrace{a[1 - \lambda(t)]}_{\text{buildup}} - \underbrace{b\lambda(t)\dot{\gamma}}_{\text{breakdown}}, \quad (3)$$

which assumes that the rate of structure breakdown is proportional to both  $\lambda$  and shear rate, whereas the rate of buildup is proportional to the broken structure  $(1-\lambda)$  but is independent of shear rate. This rate equation predicts a dynamic equilibrium when the structure parameter is:

$$\lambda_e = \frac{1}{1 + \frac{b}{a}\dot{\gamma}} \quad (4)$$

For the equation of state, Cheng and Evans<sup>8</sup> suggested a relationship which included a yield stress proportional to the structure parameter  $\lambda(t)$ :

$$\tau(t) = \lambda(t)\tau_y + [\eta_\infty + c\lambda(t)]\dot{\gamma} \quad (5)$$

Incorporation of shear-thinning properties in Eq. 5 gives the modified Cheng-Evans equation:

$$\tau(t) = \lambda(t)\tau_y + [\eta_\infty + c\lambda(t)]\dot{\gamma}^m \quad (6)$$

where  $m < 1$  is the power-law index (or flow index) for shear-thinning fluids. Accordingly, the equilibrium flow curve for the modified Cheng-Evans equation becomes:

$$\tau_e = \lambda_e\tau_y + (\eta_\infty + c\lambda_e)\dot{\gamma}^m \quad (7)$$

This is equivalent to the Herschel-Bulkley equation,<sup>9</sup> which satisfactorily represents the rheology of water-based drilling fluids.<sup>3,10</sup>

To find the parameters in the modified Cheng-Evans equation (Eq. 6), it is necessary to express  $\lambda$  as a function of shear rate. This can be done by integrating Eq. 3 and by substituting for  $\lambda_e$  from Eq. 4:

$$\lambda(t) = (\lambda_0 - \lambda_e)e^{-\frac{t}{T}} + \lambda_e, \quad (8)$$

where,

$$\frac{1}{T} = a + b\dot{\gamma} \quad (9)$$

$\lambda_0$  is the structure at time  $t = 0$ . Substitution of Eqs. 4, 8 and 9 in Eq. 6 then defines the time dependence of shear stress:

$$\tau(t) = \tau_1 e^{-\frac{t}{T}} + \tau_e, \quad (10)$$

with:

$$\tau_1 = (\lambda_0 - \lambda_e)(\tau_y + c\dot{\gamma}^m) \quad (11)$$

$$\tau_e = \lambda_e \tau_y + (\eta_\infty + c\lambda_e) \dot{\gamma}^m \quad (12)$$

Eqs. 3 and 7 may be used as the basis for a mathematical description of thixotropic behaviour in fluids. The various parameters in Eq. 7 can be determined by measuring the steady-state shear stress at a number of shear rates.

## Experiments

The test fluid was an unweighted WBM containing 64.3 g of bentonite per litre of water (22.5 lb/bbl). The fluid was prepared by adding the clay to water over a period of two minutes while shearing the suspension with a Silverson high-speed mixer. The pH of the suspension was adjusted to 9.5. The suspension was then heat-aged in a standard roller oven at 100°C for 48 hr.

The steady-shear measurements were carried out on a Bohlin VOR rheometer using a concentric cylinder measuring geometry. The yield stress measurements were performed on a Carrimed controlled-stress rheometer, using a similar geometry. Before each experiment, the material was cold-rolled for 1 hr at room temperature and at a shear rate of about 5 s<sup>-1</sup>. This had a homogenising effect on the fluid and brought all samples to similar initial shear history. After transfer to the measuring geometry of the rheometer, the samples were allowed to rest for 10 min to reach thermal equilibrium before measurements began. Sample temperature was maintained at 25°C ± 0.1°C throughout the experiment. Four types of measurements were performed:

*Stress relaxation* - Samples were sheared at a constant rate for 6-8 hr. Equilibrium stress was determined at a number of shear rates in the range 2.9–1460 s<sup>-1</sup>. Reproducibility was checked by repeating the measurements 3 – 6 times at each shear rate.

*Shear rate step-change* - Shear rate was changed several times between high and low values, and the equilibrium stress was determined at each shear rate. The results were used to establish the time- and shear-history dependence of shear stress.

*Yield stress measurements* - Shear stress was applied to the sample and increased at a controlled rate until angular displacement was detected.

*Hysteresis loops* - Shear rate was ramped up and down repeatedly over a selected range to obtain the hysteresis loops characteristic of thixotropic materials.

Sample dehydration during measurements was eliminated by placing a thin layer of a viscosity-standard oil S60 (viscosity of 102.3 cP at 25°C, supplied by Cannon Instruments, USA), on the free surface of the sample. The oil film did not affect the rheological properties of the mud sample.

## Results and Discussion

Fig. 3 shows typical stress-relaxation data at several shear rates. The data shows that faster breakdown takes place at higher shear rates, and that

the rate of breakdown decreases with increasing time. Both of these are consistent with the rate equation for structure (Eq. 3).

The validity of the single-structure rate equation for the WBM of these experiments was tested by fitting Eq. 10 to the experimental stress relaxation data using a non-analytical least-squares regression routine. With  $\tau_e$  determined directly from the measured data, the curve fitting gave unique values for  $\tau_1$  and  $T$ . The fitted curves are shown as solid lines in Fig. 3. Although the general fit is good, it seems that the function does not describe the data satisfactorily at early times in the experiments. This may suggest that in the stress-relaxation experiments, there is a fast viscous drag-driven structure breakdown (to flocs and aggregates) followed by a slower breakdown caused by the collision of mobile flocs and aggregates. Because the population of data points is heavier toward the steady state, it is mostly the behaviour of the slower process that is reflected in the fitted function. The quality of the fit may be improved by either using a weighted curve fitting or by using a double-exponential function to describe shear stress. The latter is discussed further in a later section.

The pre-exponential coefficients  $\tau_1$  obtained from the above curve fitting are plotted against  $\dot{\gamma}$  in Fig. 5 and show strong shear-thinning characteristics.

### Time-Dependence of Shear Stress

The relaxation times  $T$  obtained from the above curve fitting are plotted as  $T^{-1}$  vs.  $\dot{\gamma}$  in Fig. 6. According to the single-structure theory, a plot of  $T^{-1}$  vs.  $\dot{\gamma}$  is a straight line with slope  $b$ , and intercept  $a$  on the  $T^{-1}$ -axis (Eq. 9). The data in Fig. 6, however, has two distinctly different slopes at low and at high shear rates. A method advocated by many for determining the time dependence of shear stress is the high-low shear rate step-change measurements illustrated in Fig. 4. Using Eq. 10, a least-squares regression of data at any high-low shear-rate pair gives the time constants for the net structure breakdown and buildup,  $T_1$  and  $T_2$ , respectively:

$$\frac{1}{T_1} = a + b\dot{\gamma}_1 \quad (13)$$

$$\frac{1}{T_2} = a + b\dot{\gamma}_2, \quad (14)$$

The range of shear rates used in the step-change measurements was 100–1500 s<sup>-1</sup>. The results are presented in Table 1 as the relaxation times of the breakdown (low-to-high shear rate) and buildup (high-to-low shear rate) processes. The relaxation times to the left of the diagonal belong to net buildup of structure, while those to the right of the diagonal represent net breakdown. The results suggest that the buildup of structure is a slower process than the breakdown. In one case, shear rate pair 91.9 and 146.1 s<sup>-1</sup>, the close proximity of the two shear rates made calculation of relaxation times subject to large errors.

For each pair of relaxation times, Eqs. 13 and 14 were solved simultaneously to find the constants  $a$  and  $b$ . These are given in Table 2 for five pairs of shear rates. Due to the wide variation in the  $b/a$  ratio, the time dependence of the fluid cannot be described adequately by a single relationship over the entire shear-rate range. A better

approximation may be obtained by fitting two straight lines to the  $T^{-1}$  vs.  $\dot{\gamma}$  data. For shear rates in the range 0–100 s<sup>-1</sup>:

$$\frac{1}{T} = 1.5 \times 10^{-5} + 4.8 \times 10^{-6} \dot{\gamma}, \quad \text{for } 0-100 \text{ s}^{-1} \quad (15)$$

$$\frac{1}{T} = 1.5 \times 10^{-4} + 7.0 \times 10^{-7} \dot{\gamma}, \quad \text{for } 100-1500 \text{ s}^{-1} \quad (16)$$

The straight lines in Fig. 6 are graphical representations of the above relationships. In the absence of a single description for relaxation time in the range of shear rates used here, the  $b/a$  ratio will be determined by curve fitting to the equilibrium shear stress data.

### Shear-History Dependence of Shear Stress

Description of structure as a function of time requires an expression for  $\lambda_0$ , which represents the shear-history dependence of rheological properties.  $\lambda_0$  cannot be measured directly but it may be determined in terms of  $\tau_1$ , the pre-exponential coefficient in Eq. 10. It can be shown that differentiation of Eqs. 8, 9 and 12, followed by elimination of  $d\tau(t)/dt$  and  $d\lambda(t)/dt$ , can lead to the following expression for  $\lambda_0$ :

$$\lambda_0 - \lambda_e = \frac{k_1 \dot{\gamma}}{(1 + k_2 \dot{\gamma})(\tau_y + c \dot{\gamma}^m)} \quad (17)$$

In the above,  $k_1$  and  $k_2$  are constants of an empirical equation that describes adequately the  $\tau_1$  vs.  $\dot{\gamma}$  data presented in Fig. 5:

$$\tau_1 = \frac{k_1 \dot{\gamma}}{1 + k_2 \dot{\gamma}} \quad (18)$$

The constants were obtained by curve fitting of Eq. 18 to the  $\tau_1$  vs.  $\dot{\gamma}$  data, and were found to be  $k_1=0.145$ ,  $k_2=0.00516$ .

### Parameters in Equilibrium Flow Curve

The remaining parameters,  $\tau_y$ ,  $b/a$ ,  $\eta_\infty$ ,  $c$  and  $m$  in Eq. 7 are determined by a combination of curve fitting and direct measurements. The direct measurements reduce the number of parameters determined by curve fitting so that a unique “best fit” can be determined.

The viscosity of the unstructured fluid,  $\eta_\infty$ , can be determined by assuming that the drilling fluid behaves like a Bingham fluid at high shear rates (*i.e.* where  $m \approx 1$ ), and that the  $\tau_e$  vs.  $\dot{\gamma}$  data in that region can be approximated by a straight line ( $\lambda_0 \approx 0$ ). The slope of the high-shear asymptote will then give  $\eta_\infty$ . Fitting a straight line through the equilibrium stress data above  $\dot{\gamma} = 500 \text{ s}^{-1}$  (dashed line in Fig. 7) gives  $\eta_\infty = 0.02 \pm 0.002$ , with units Pa·s<sup>m</sup> consistent with Eq. 7.

The yield stress was determined by applying a known shear stress to the sample and observing the rate of angular displacement. The stress at which displacement was detected was taken as the yield stress. The measurements were repeated several times, and a reproducible value of  $\tau_y = 16.0 \text{ Pa}$  was obtained (Fig. 8). This value was adopted as the yield stress corresponding to the initial structural state of the fluid as used in all the experiments.

Substituting for  $\eta_\infty = 0.02 \text{ Pa}\cdot\text{s}^m$  and  $\tau_y = 16.0 \text{ Pa}$ , the steady-state Cheng-Evans equation (Eq. 7) becomes:

$$\tau_e = \frac{16.0}{1 + \frac{b}{a} \dot{\gamma}} + \left(0.02 + \frac{c}{1 + \frac{b}{a} \dot{\gamma}}\right) \dot{\gamma}^m \quad (19)$$

The three parameters  $c$ ,  $b/a$  and  $m$  have to be determined by least-squares regression of equilibrium stress data to Eq. 19. However, it was found that parameters  $c$  and  $b/a$  exhibit high sensitivity to small variations in  $m$ . For example, a 1% change in  $m$  produces 20% and 30% changes in  $c$  and  $b/a$ , respectively. As a result, Eq. 19 does not give a unique best fit to the equilibrium data. Since parameters  $c$  and  $b/a$  have similar mutual sensitivities, it is necessary to force the value of  $m$  in Eq. 19.

In the family of the best fits obtained by least-squares regression of the equilibrium data, the value of  $m$  varies from 0.642 to 0.985. Assuming an average value of  $m=0.81$ , Eq. 19 can be forced to produce singular values for  $b/a$  and  $c$ :

$$\frac{b}{a} = 5.44 \times 10^{-4} \pm 9.46 \times 10^{-5} \quad (20)$$

$$c = 0.20 \pm 0.015 \quad (21)$$

The fitted curve represented by these parameters is shown by a solid line in Fig. 7.

The complete set of relationships produced for describing the time- and shear-history dependence of the rheological properties of the water-based fluid of these experiments is as follows:

$$\tau(t) = \tau_y \lambda(t) + [\eta_\infty + c \lambda(t)] \dot{\gamma}^m \quad (22)$$

$$\lambda(t) = (\lambda_0 - \lambda_e) e^{-\frac{t}{T}} + \lambda_e, \quad (23)$$

With:

$$\lambda_e = \frac{1}{1 + \frac{b}{a} \dot{\gamma}}, \quad (24)$$

$$\lambda_0 - \lambda_e = \frac{k_1 \dot{\gamma}}{(1 + k_2 \dot{\gamma})(\tau_y + c \dot{\gamma}^m)}, \quad (25)$$

The time dependence is further defined by the following expressions:

$$\frac{1}{T} = 1.5 \times 10^{-5} + 4.8 \times 10^{-6} \dot{\gamma}, \quad \text{for } 0-100 \text{ s}^{-1} \quad (26)$$

$$\frac{1}{T} = 1.5 \times 10^{-4} + 7.0 \times 10^{-7} \dot{\gamma} \quad \text{for } 100-1500 \text{ s}^{-1} \quad (27)$$

The parameters in the above equations are summarized below:

$$\begin{aligned}\tau_y &= 16.0 \text{ Pa} \\ \eta_\infty &= 0.02 \text{ Pa}\cdot\text{s}^m \\ c &= 0.20 \text{ Pa}\cdot\text{s}^m \\ m &= 0.81 \\ b/a &= 5.44 \times 10^{-4} \text{ s} \\ k_1 &= 0.145 \text{ Pa}\cdot\text{s} \\ k_2 &= 0.00516 \text{ s}\end{aligned}$$

For the model to give a good prediction of thixotropic behaviour, one of the following initial conditions must be satisfied:

- Material initially sheared at a high rate so that  $\lambda_0 \approx 0$ . This corresponds to the condition of the drilling fluid as it issues at the drill bit, where it is subjected to shear rates on the order  $10^5 \text{ s}^{-1}$ .
- Fluid at equilibrium at a finite shear rate such that  $\lambda_0 = \lambda_c$ . This condition may correspond to the state of the fluid in the circulation system at the surface.
- Material initially at rest, corresponding to a break in fluid circulation. In this situation, one may assume that the initial conditions are similar to those of the fluid in this study. Or, if there has been an extended break in circulation, it may be assumed that the fluid has a fully formed structure, i.e.  $\lambda_0 = 1$ .

### Model Validation

Validity of the model and the accuracy of the final curve fitting can now be tested by attempting to predict the hysteresis loops produced when shear rate is ramped. If the fluid is subjected to a sequence of shear rates  $\dot{\gamma}_i$ , for a period  $t_i$  at each shear rate, the structure  $\lambda_i$  at the end of interval  $i$  becomes the initial structure for the next interval at shear rate  $\dot{\gamma}_{i+1}$ , i.e.  $\lambda_{0,i+1} = \lambda_i$ .

The experimental data in Fig. 9 were obtained by ramping the shear rate up and then down over the range 11.6–1460  $\text{s}^{-1}$ . The cycle was repeated five times. The total ramp time in each direction was 48 min, equivalent to 20 readings at 144-second intervals. The fluid was pre-treated as described earlier. The solid lines in Fig. 9 show the calculated hysteresis loops. The model does not predict the first cycle satisfactorily. This is expected because, as discussed earlier, the single-exponential time dependence does not fit the stress relaxation data well at early times. However, as time progresses, i.e. as the cycle is repeated, the agreement between the experimental and predicted values improves. The maximum difference between the measured stress values and those predicted by the model for the final loop is about 7%. This value decreases as the ramp time is increased.

The slopes of the “up” and “down” curves are determined to a large extent by the value of parameter  $m$ . It appears that the assumed average value of  $m=0.81$  produces good agreement with the experimental data.

### Alternative Thixotropy Models

Evidence from these experiments suggests that the thixotropic behaviour of water-based muds may be better described by two rate processes with distinctly different relaxation times. In this scheme, the first process may be a fast, viscous drag-driven breakdown, which breaks the intact (house-of-cards) structure into flocs and aggregates. The second process has a slower but longer-term effect, causing further breakdown by promoting collision between the mobile flocs and

aggregates. The two structural processes may be assumed to occur in series. This would lead to double-exponential functions for the description of structure and shear stress, of the type:

$$\lambda(t) = \lambda_1 e^{-\frac{t}{\tau_1}} + \lambda_2 e^{-\frac{t}{\tau_2}} + \lambda_e \quad (35)$$

Mathematical derivations leading to the time-description of structure have been made for this model, and it appears that the five coefficients involved in Eq. 35 are complicated functions of shear rate which do not lend themselves to determination by simple optimization procedures. This makes the two-structure model unsuitable for engineering applications.

### Engineering Application

The model was used to estimate the gel values of the test fluid for comparison against those measured at 77°F (25°C) following the API viscometric procedure. In the measurement procedure, the fluid is sheared at 600 rpm until a steady dial reading is obtained, at which time shearing is stopped and the fluid is allowed to rest for a specified period (10 sec, 10 min, and occasionally 30 min) before it is sheared again at 3 rpm (5.1  $\text{s}^{-1}$ ). The maximum dial reading is then recorded as the 10-sec, 10-min or 30-min gel value. To simulate the measurement procedure, it is assumed that the high-speed shearing destroys fluid structure completely, thus  $\lambda_0 = 0$  at  $t=0$ . Further, during the gelling period, little or no structure breakup is expected, therefore, only the structure-buildup term of Eq. 3 is used. This results in the following equation for gel development:

$$\lambda(t) = 1 - e^{-at} \quad (36)$$

For constant  $a$ , the lowest value from Table 2 was used which corresponded to lower shear rates. A plot of the estimated structure development for the test fluid of these experiments is shown in Fig. 10. The data suggest 0.4% structure after 10 sec, 24% after 10 min and 52% after 30 min. It takes more than 4 hr for the structure to become fully developed.

Using the above structure estimates, the 10-sec, 10-min and 30-min gel values were calculated to be 0.1, 4.1, 8.8 lb/100  $\text{ft}^2$ , respectively. The corresponding measured values were 1.5, 4 and 7 lb/100  $\text{ft}^2$ . There appears to be good agreement in the two longer-term gels.

For engineering applications, the steps involved in characterizing the thixotropic properties of WBM may be simplified to some extent by using oilfield-type rheometers. However, this has to be a device that allows low shear-rate measurements. A main challenge is in the determination of pre-exponential coefficient  $\tau_1$  in Eq. 10. For this, shear stress should be measured as a function of time at several shear rates, thus requiring a rheometer capable of logging shear stress vs. time.

The following steps may be taken to determine the time- and shear-dependence of structure:

- Measure rheology at several shear rates, allowing time for values to reach steady state. This will be the equilibrium flow curve.
- Determine  $\eta_\infty$  from the slope of the high-shear asymptote to the flow curve.

- If direct measurement of yield stress is not an option, then calculate  $\tau_y$  by fitting a Herschel-Bulkley equation to the flow curve.
- Approximate  $m$  by using the flow index of the Herschel-Bulkley equation. Determine the constants  $c$  and  $b/a$  by curve fitting Eq. 19 to the equilibrium flow curve.
- Measure shear stress as a function of time at several shear rates. Curve fitting of Eq. 10 to the data at each shear rate will provide the required  $\tau_t$  vs.  $\dot{\gamma}$  data. The  $\tau_t$  vs.  $\dot{\gamma}$  data together with Eq. 18 will give constants  $k_1$  and  $k_2$ .

Eqs. 22-27 may then be used to characterize thixotropy for engineering calculations. Depending on the fluid system being used, the relaxation times (Eqs. 26-27) may have to be redefined.

### Conclusions

The thixotropic characteristics of some drilling fluids may have a significant effect on their rheological properties in the time scale and range of shear rates encountered around the wellbore. Hitherto, the effect has been accounted for in fluid design and engineering calculations by the 10-sec and 10-min gel values measured routinely in drilling fluid laboratories. The results of this work show that relatively simple semi-empirical models, based on a single-structure theory, may be devised in such a way that the effects of time and shear history on rheology can be incorporated in engineering calculations.

Although this model is based on an unweighted bentonite suspension, similar work on weighted muds may be carried out in order to study the effect of added solids on thixotropic behaviour. There is scope for further work to determine the temperature dependence of such behaviour, as well as its nature and effect in turbulent flows.

### Acknowledgments

The author thanks M-I SWACO for permitting the publication of this work.

### References

1. Jenekhe, S.A., Davis, H.T. and Scriven, L.E. "Cold Stage Scanning Electron Microscopy of Bentonite Suspensions." 38th Annual Proceedings of Electron Microscopy Society of America, (Ed. G.W. Bailey), San Francisco, California, (1989) 206.
2. Dairanieh, I.S. and Lahalih, S.M. "Novel Polymeric Drilling Mud Viscosifiers." *European Polymer Journal*, v.24 (1988) 831.
3. Alderman, N.J., Ram Babu, D., Hughes, T.L. and Maitland, G.C. "The Rheological Properties of Water-Based Drilling Fluids." 10<sup>th</sup> International Congress on Rheology, Sydney, August 14-19, 1988.
4. Annis, M.R., "High-Temperature Flow Properties of Water-Based Drilling Fluids." *Journal of Petroleum Technology*, v19, no.8, (1967) 1074.
5. Hiller, K.H. "Rheological Measurements on Clay Suspensions and Drilling Fluids at High Temperatures and Pressures." *Journal of Petroleum Technology*, v.15, no.7 (1963) 779.

6. Mercer, H.A. and Weymann, H.D. "Structure of Thixotropic Suspensions in Shear Flow. III. Time-Dependent Behaviour." *Transactions of the Society of Rheology*, v.82, no.1, (1974) 199.
7. Dolz, M., Jiménez, J., Jesús Hernández, M., Delegido, J. and Casanovas, A. "Flow and Thixotropy of non-Contaminating Oil Drilling Fluids Formulated with Bentonite and Sodium Carboxymethyl Cellulose." *Journal of Petroleum Science and Engineering*, v.57 (2007) 294-302.
8. Cheng, D.C.-H. and Evans, F. "Phenomenological Characterisation Of The Rheological Behaviour of Inelastic Reversible Thixotropic and Anti-Thixotropic Fluids." *British Journal of Applied Physics*, v.16 (1965) 1599.
9. Herschel, W.H and Bulkley, R. "Measurement of Consistency as Applied to Rubber-Benzene Solutions." *Proceedings of the American Society for Testing and Materials*, v.26, (1926) 621.
10. Zamora, M. and Lord, D.L. "Practical Analysis of Drilling Mud Flow in Pipes and Annuli." SPE 4976, SPE Annual Fall Meeting, Houston, October 6-9, 1974.

Table 1. Relaxation Times of Structure Breakdown and Buildup Processes				
Shear rate (s <sup>-1</sup> )	To			
From	91.9	146.1	461.0	1460.0
91.9	-	-	608	143
146.1	-	-	661	331
461.0	1550	1060	-	671
1460.0	1060	1230	910	-

Table 2. Rate Constants for Structure Breakdown and Buildup Processes			
Shear Rates (s <sup>-1</sup> )	a (s <sup>-1</sup> )	b	b/a (s)
91.9 ↔ 461.0	4.0×10 <sup>-4</sup>	2.7×10 <sup>-6</sup>	0.0068
91.9 ↔ 1460.0	6.5×10 <sup>-4</sup>	4.3×10 <sup>-6</sup>	0.0066
146.1 ↔ 461.0	6.8×10 <sup>-4</sup>	1.8×10 <sup>-6</sup>	0.0026
146.1 ↔ 1460.0	5.7×10 <sup>-4</sup>	1.7×10 <sup>-6</sup>	0.0029
461.0 ↔ 1460.0	9.2×10 <sup>-4</sup>	0.4×10 <sup>-6</sup>	0.0004

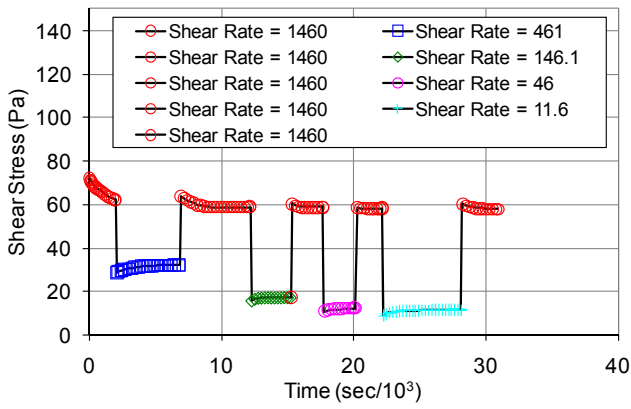


Figure 1. Shear rate step-change tests.

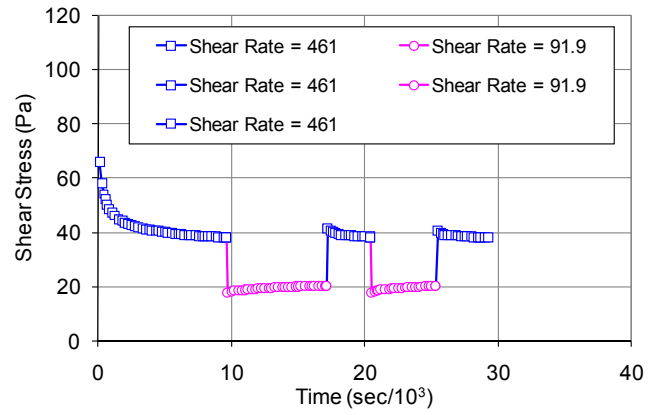


Figure 4. Shear rate step-change tests.

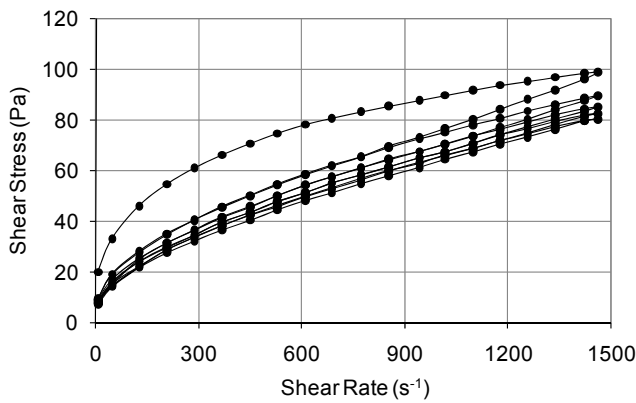


Figure 2. Hysteresis loops demonstrating thixotropic behaviour.

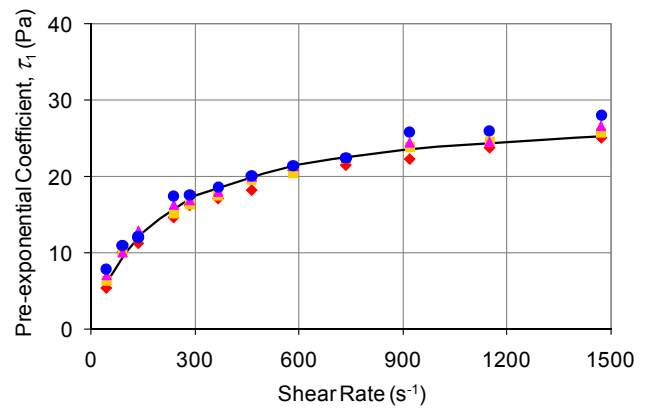


Figure 5. Pre-exponential coefficients from a single-exponential fit to stress-relaxation data.

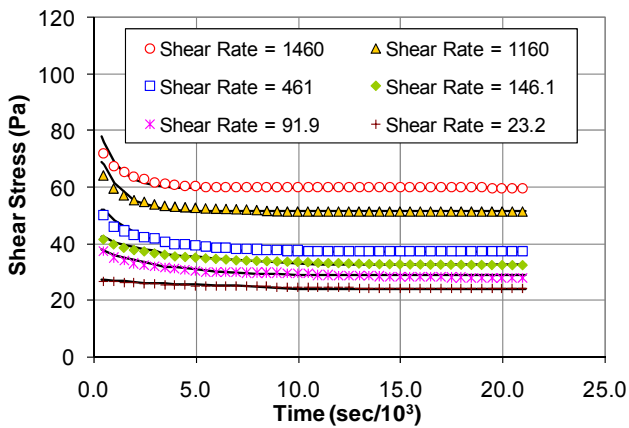


Figure 3. Steady-shear stress-relaxation data.

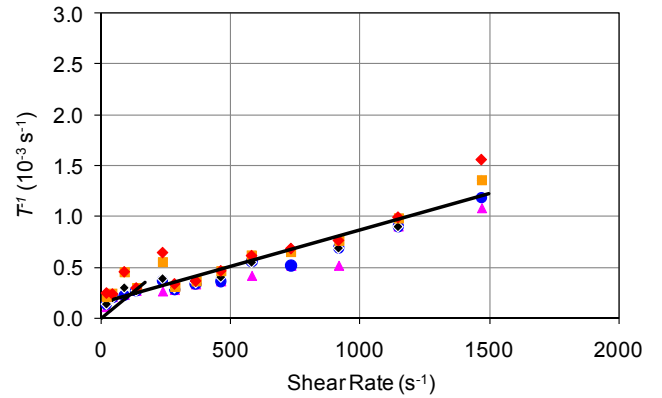


Figure 6. Inverse relaxation time vs. shear rate for stress-relaxation experiments.

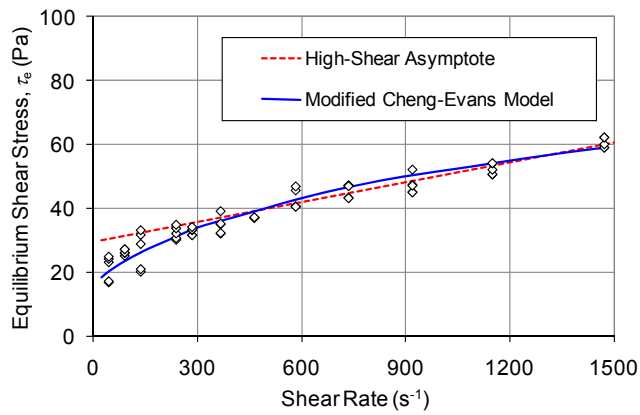


Figure 7. Illustration of the high-shear asymptote and the modified Moore-Cheng model.

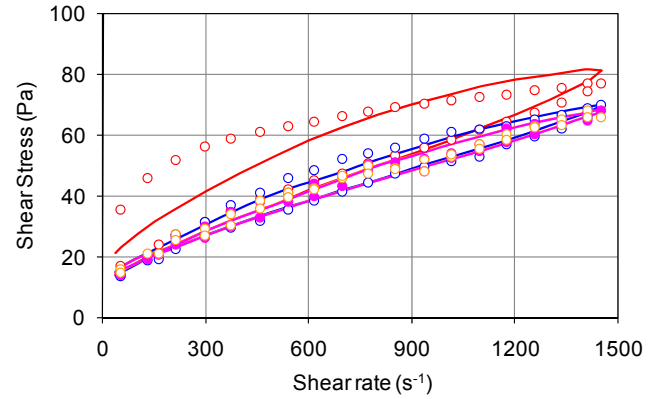


Figure 9. Hysteresis loops produced by ramping the shear rate in the range 14.6-1460 s<sup>-1</sup>.

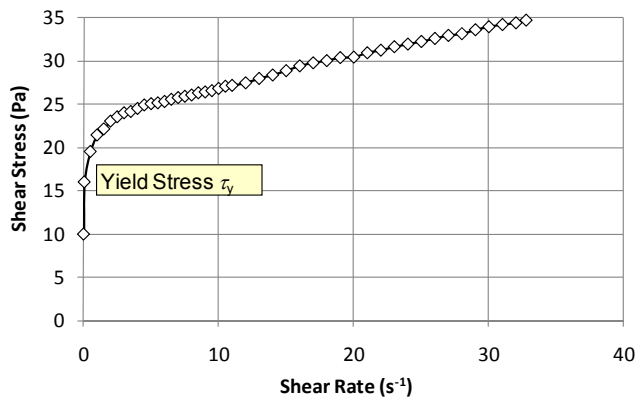


Figure 8. Determination of the yield stress on the controlled-stress rheometer.

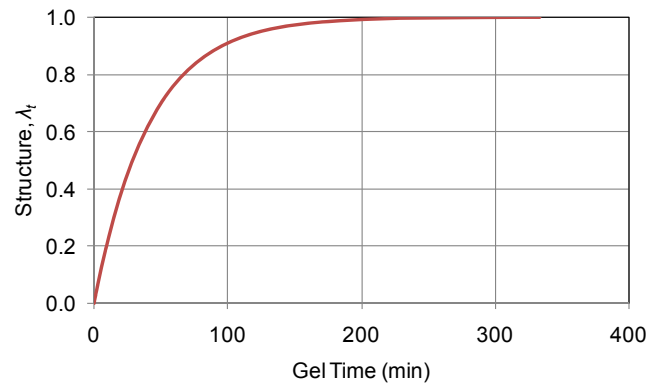


Figure 10. Structure buildup after high-speed shearing of WBM.